CYCLOSTATIONARITY-BASED BLIND CLASSIFICATION OF ANALOG AND DIGITAL MODULATIONS

Octavia A. Dobre[1], Ali Abdi[2], Yeheskel Bar-Ness[2], and Wei Su[3]
[1]Faculty of Eng. and Applied Science, Memorial University of Newfoundland, St. John's, NL A1B 3X5, Canada
[2]CCSPR, Dept. of ECE, New Jersey Institute of Technology, Newark, NJ 07102, USA
[3]RDECOM, Fort Monmouth, NJ 07703, USA
dobre@engr.mun.ca, abdi@adm.njit.edu, barness@yegal.njit.edu, wei.su@us.army.mil

Abstract *- The problem of blind analog and digital modulation classification is tackled in this paper. A cyclostationarity-based classifier is proposed, which does not require estimation of carrier phase and frequency offset, signal and noise powers, and timing recovery as preprocessing tasks. Numerical simulations are performed to validate theoretical developments.*

I. INTRODUCTION

Blind modulation classification (MC) is a major task of an intelligent receiver, with both military and commercial applications [1]. A modulation classifier essentially involves two steps, i.e., signal preprocessing and modulation recognition. Preprocessing tasks may include estimation of carrier phase and frequency offset, signal and noise powers, timing recovery, etc. Depending on the classification algorithm employed in the second step, different preprocessing tasks can be required. Classification algorithms which rely less on preprocessing are sought. Research on MC has been carried out for at least a decade [1]-[9]. Many algorithms proposed in the literature address the digital modulation classification problem [1]-[5]. A survey of such classification techniques is presented in [1]. Nonetheless, classification of analog and digital modulations is of interest, as some existing systems still use analog communication techniques. Algorithms for the recognition of analog and digital modulations are also proposed in the literature [5]-[8]. However, the performance of most of these algorithms is presented under the assumption of perfect preprocessing, and it can substantially degrade with model mismatches, such as carrier phase and frequency offset.

In this paper, we propose a novel algorithm, which exploits signal cyclostationarity for analog and digital modulation classification. The algorithm does not require estimation of carrier phase, frequency offset, signal and noise powers, and timing recovery in the preprocessing step, and is applicable to the following pool of modulations: amplitude modulation (AM), double sideband (DSB), single sideband (SSB), *M*-ary phase shift keying (*M*-PSK) and *M*-ary quadrature amplitude modulation (*M*-QAM).

The rest of the paper is organized as follows. The signal model and corresponding statistical characterization are presented in Section II, the proposed cyclostationarity-based classification algorithm is introduced in Section III, simulation results are given in Section IV, and conclusions are drawn in Section V. Temporal cyclostationarity parameters are defined in Appendix A, and results for the first- and/ or second-order cyclostationarity of the signals of interest are derived in Appendix B.

II. SIGNAL MODEL AND CORRESPONDING STATISTICAL CHARACTERIZATION

A. Signal Model

Let the received baseband waveform $r^{(i)}(t)$ be the sum

$$r^{(i)}(t) = e^{j\theta} e^{j2\pi\Delta f_c t} s^{(i)}(t) + w(t), \qquad (1)$$

where θ is the carrier phase, Δf_c is the carrier frequency offset, $s^{(i)}(t) = s_I^{(i)}(t) + js_Q^{(i)}(t)$ is the transmitted signal with modulation i, $w(t) = w_I(t) + jw_Q(t)$ is zero-mean complex Gaussian noise of power N, with indexes I and Q standing for in-phase and quadrature, respectively, and $j = \sqrt{-1}$. The in-phase and quadrature noise components, $w_I(t)$ and $w_Q(t)$, are zero-mean uncorrelated Gausssian processes, and uncorrelated with $s^{(i)}(t)$.

The transmitted signal is given by $s^{(i)}(t) = A(1+\mu_A x(t))$ for *i*=AM, $s^{(i)}(t) = Ax(t)$ for *i*=DSB, $s^{(i)}(t) = A(x(t) \pm j\underset{\sim}{x}(t))$ for *i*=SSB, and $s^{(i)}(t) = A\sum_k s_k^{(i)} p_{TX}(t-kT-\varepsilon T)$ for *i*=*M*-PSK and *M*-QAM, where A is the signal amplitude, μ_A is the modulation index, $x(t)$ is the zero-mean real-valued band-limited modulating signal, $\underset{\sim}{x}(t)$ is the Hilbert transform of $x(t)$, $p_{TX}(t)$ is the transmit pulse shape, T is the symbol period, εT represents a timing error, with $0 \le \varepsilon < 1$, $s_k^{(i)} = s_{k,I}^{(i)} + js_{k,Q}^{(i)}$ is the symbol transmitted within the k th period, drawn from the signal constellation i, *i*=*M*-PSK and *M*-QAM, and M is the number of points in the signal constellation [10]. The data symbols $\{s_k^{(i)}\}$ are assumed to be zero-mean independent and identically distributed random variables, with $\{s_{k,I}^{(i)}\}$ and $\{s_{k,Q}^{(i)}\}$ uncorrelated.

At the receive-side, normalization of the signal is carried out with respect to the received signal power to remove any scale factor from data, and then, sampling is performed at a sampling rate f_s (no aliasing occurs [11]). The normalized discrete-time signal is $r^{(i)}(k) := r^{(i)}(t)/\sqrt{S+N}\,|_{t=kf_s^{-1}}$, with S as the signal power.

B. Cyclostationarity of Signals of Interest

Results derived in Appendix B for the first- and/or second-order cyclic temporal cumulant functions (CTCFs)[1] of the signals of interest are presented in the sequel, with emphasis on their application to modulation classification.

The first-order/ zero-conjugate CTCFs[1] of AM, DSB, SSB, *M*-PSK, and *M*-QAM normalized discrete-time received signals, at cycle frequency (CF) β, are as follows,

$$c_{r^{(\mathrm{AM})}}(\beta)_{1,0} = Ae^{j\theta}(S+N)^{-1/2}, \text{ with } \beta = \Delta f_c f_s^{-1}, \tag{2}$$

and

$$c_{r^{(i)}}(\beta)_{1,0} = 0, \text{ any } \beta,\ i = \text{DSB, SSB, } M\text{-PSK, } M\text{-QAM}. \tag{3}$$

One can thus conclude that the received AM signal exhibits first-order cyclostationarity, whereas all other signals of interest do not. This property of the AM signal is exploited for its recognition.

The second-order/ zero-conjugate CTCFs[1] of DSB, SSB, *M*-PSK, *M*-QAM, $M \geq 4$, and BPSK normalized discrete-time received signals, at CF β and delay τ, are as follows,

$$c_{r^{(\mathrm{DSB})}}(\beta;\tau)_{2,0} = A^2(S+N)^{-1}e^{j2\theta}e^{j2\pi\Delta f_c \tau f_s^{-1}}m_x(\tau f_s^{-1})_{2,0}, \tag{4}$$

with $\beta = 2\Delta f_c f_s^{-1}$, and $m_x(\tau f_s^{-1})_{2,0}$ as the second-order/ zero-conjugate moment of $x(k) = x(t)|_{t=kf_s^{-1}}$,

$$c_{r^{(i)}}(\beta;\tau)_{2,0} = 0, \text{ any } \beta,\ i = \text{SSB, } M\text{-PSK, } M\text{-QAM, } M \geq 4, \tag{5}$$

and

$$c_{r^{(\mathrm{BPSK})}}(\beta;\tau)_{2,0} = A^2(S+N)^{-1}T^{-1}f_s^{-1}e^{-j2\pi\gamma f_s \varepsilon T} \times e^{j2\theta}e^{j2\pi\Delta f_c \tau f_s^{-1}}\sum_{k=-\infty}^{\infty} p_{TX}(k)p_{TX}(k+\tau)e^{-j2\pi\gamma k}, \tag{6}$$

with $\beta = \gamma + 2\Delta f_c f_s^{-1}$, $\gamma = f_s^{-1}k/T$, k integer[2], and $p_{TX}(k) = p_{TX}(t)|_{t=kf_s^{-1}}$.

Thus, for *i*=DSB and BPSK, $c_{r^{(i)}}(\beta;\tau)_{2,0} \neq 0$ at CFs $\beta = 2\Delta f_c f_s^{-1}$ and $2\Delta f_c f_s^{-1} + f_s^{-1}k/T$ [2], respectively, whereas for *i*=SSB, *M*-PSK, and *M*-QAM, $M \geq 4$, $c_{r^{(i)}}(\beta;\tau)_{2,0} = 0$, any β. This property is exploited here to distinguish between DSB, BPSK and SSB, *M*-PSK, *M*-QAM, $M \geq 4$.

The second-order/ one-conjugate CTCFs[1] of DSB, SSB, *M*-PSK and *M*-QAM normalized discrete-time received signals, at CF β and delay τ, are as follows

$$c_{r^{(\mathrm{DSB})}}(\beta;\tau)_{2,1} = 2A^2(S+N)^{-1}e^{-j2\pi\Delta f_c \tau f_s^{-1}}m_x(\tau f_s^{-1})_{2,1} + c_w(\beta;\tau)_{2,1}, \tag{7}$$

with $\beta = 0$, $m_x(\tau f_s^{-1})_{2,1}$ as the second-order/ one-conjugate moment of $x(k)$, and $c_w(\beta;\tau)_{2,1}$ as the of second-order/ one-conjugate cyclic cumulant of $w(k) = w(t)/\sqrt{S+N}|_{t=kf_s^{-1}}$, at CF β and delay τ,

$$c_{r^{(\mathrm{SSB})}}(\beta;\tau)_{2,1} = 2A^2(S+N)^{-1}e^{-j2\pi\Delta f_c \tau f_s^{-1}} \times (m_x(\tau f_s^{-1})_{2,1} \mp j\underset{\smile}{m}_x(\tau f_s^{-1})_{2,1}) + c_w(\beta;\tau)_{2,1}, \tag{8}$$

with $\beta = 0$, and $\underset{\smile}{m}_x(.)_{2,1}$ as the Hilbert transform of $m_x(.)_{2,1}$, and

$$c_{r^{(i)}}(\beta;\tau)_{2,1} = A^2(S+N)^{-1}T^{-1}f_s^{-1}e^{-j2\pi\gamma f_s \varepsilon T}e^{-j2\pi\Delta f_c \tau f_s^{-1}} \times \sum_{k=-\infty}^{\infty} p_{TX}(k)p_{TX}^{*}(k+\tau)e^{-j2\pi\gamma k} + c_w(\beta;\tau)_{2,1}, \tag{9}$$

with $\beta = \gamma = f_s^{-1}k/T$, k integer[2], *i*=*M*-PSK, *M*-QAM, $M \geq 2$, and * as the complex conjugate.

Thus, for $i =$ DSB and SSB, $c_{r^{(i)}}(\beta;\tau)_{2,1} \neq 0$ at $\beta = 0$ only, whereas for *i*=*M*-PSK, *M*-QAM, $M \geq 2$, $c_{r^{(i)}}(\beta;\tau)_{2,1} \neq 0$ at $\beta = f_s^{-1}k/T$, k integer[2]. This property is exploited to distinguish between DSB and BPSK, as well as between SSB and *M*-PSK, *M*-QAM, $M \geq 4$.

III. Proposed Cyclostationarity-Based Classifier

The binary decision tree algorithm proposed for blind recognition of analog and digital modulations is depicted in Fig. 1. At each node of the tree, signal cyclostationarity is exploited to make a decision on the modulation format of the received signal.

A. Binary Decision-Tree Classification Algorithm

At Node 1 of the tree, discrimination between AM and DSB, SSB, *M*-PSK, *M*-QAM, $M \geq 2$, is performed, by exploiting the presence of a CF in the first-order/ zero-conjugate CTCF of the AM signal. The recognition process is blindly performed, consisting of the following two steps:

Step I: The magnitude of the first-order/ zero-conjugate CTCF is estimated from the finite length received data sequence, at candidate CFs, β's, over the $[-1/2, 1/2)$ range. For an AM signal, a peak occurs in this magnitude at CF $\beta = \Delta f_c f_s^{-1}$, and its value decreases with a reduction in the signal to noise ratio (SNR), defined as SNR:= S/N (see (2)). Thus, below a certain SNR, the value of this peak becomes comparable with the statistically insignificant spikes, which appear in the estimated CTCF magnitude at candidate CFs $\beta' \neq \beta$, due to the finite length of data sequence[3] (examples are provided for illustration in Section IV). If a peak is detected in the estimated magnitude of the first-order/ zero-conjugate CTCF, Step II is applied to the candidate CF corresponding to this peak. Otherwise, it is decided that the modulation format is not AM.

Step II: The cyclostationarity test developed in [12] is used to test the candidate CF corresponding to the peak detected in Step I.

---

[1] Definition of the temporal cyclostationarity parameters is given in Appendix A.

[2] Note that the integer k takes values in a denumerable set, which depends on the cyclostationarity order and signal bandwidth [2].

[3] Apparently, with a finite length data sequence, neither the first-order estimated CTCF of AM at candidates $\beta' \neq \beta$, nor of DSB, SSB, *M*-PSK, *M*-QAM, $M \geq 2$, at any candidate CF β', are identically zero. Note that results of Appendix B need to be understood as asymptotical values, which are obtained by averaging over an infinite-time interval.

Details on this test are given in Section III. B. If the tested candidate CF, β', is decided to be indeed a CF, β, the signal is identified as AM; otherwise, as belonging to the DSB, SSB, *M*-PSK, *M*-QAM signal class.

At Node 2, discrimination between DSB, BPSK, and SSB, *M*-PSK, *M*-QAM, $M \geq 4$, is performed, by exploiting the presence of a CF in the second-order/ zero-conjugate CTCF of the DSB and BPSK signals, for zero delay ($\tau = 0$). The classification process is similar to that for Node 1.

At Node 3 and Node 4, discrimination between DSB and BPSK, and SSB and *M*-PSK, *M*-QAM, $M \geq 4$, is respectively performed, by exploiting the presence of non-zero CFs in the second-order/ one-conjugate CTCF of *M*-PSK and *M*-QAM signals, $M \geq 2$, for zero-delay ($\tau = 0$). The classification process is similar to that for Node 1, with Step I applied to the sixth-order/ three-conjugate cyclic temporal moment function (CTMF), and Step II to the second-order/ one-conjugate CTCF. The second-order/ one-conjugate CTCF magnitude is not used in Step I, as its value at non-zero CFs $\beta = \pm f_s^{-1}/T$ is low even at high SNR, and peaks corresponding to these CFs cannot be distinguished from the statistically insignificant spikes which appear due to estimation based on a finite length data sequence. Instead, the two symmetric peaks are identified from the sixth-order/ three-conjugate CTMF magnitude[4]. The candidate CF which corresponds to the highest peak out of the two is then tested in Step II.

It is to be noted that the classification process does not require knowledge of the carrier phase, frequency offset, signal and noise powers, and timing recovery. In addition, it is to be noted that classification beyond Node 4 can be performed by applying other algorithms proposed in literature, such as [1]-[3] for linear digital modulations, and [7] for SSB signals.

B. Cyclostationarity Test

As mentioned in Section III. A, the cyclostationarity test developed in [12] is used to check the presence of a CF at each node l, $l = 1,...,4$, of the proposed classification algorithm. The test is formulated as a two hypothesis-testing problem, i.e., H_0: the tested candidate CF β' is not a CF, and H_1: the tested candidate CF β' is indeed a CF. The test consists of three steps, and is applied here for zero delay[1,5], as follow.
Step 1: The *n*th-order/ *q*-conjugate CTCF[5] is estimated from K samples, at the candidate CF β' selected in Step I, and for zero delay, i.e., $\hat{c}^{(K)}_{r^{(i)}}(\beta';\mathbf{0})_{n,q}$ [1,5]. Then, the vector

$$\hat{\mathbf{c}}^{(K)}_{r^{(i)},n,q} := [\mathrm{Re}\{\hat{c}^{(K)}_{r^{(i)}}(\beta';\mathbf{0})_{n,q}\} \;\; \mathrm{Im}\{\hat{c}^{(K)}_{r^{(i)}}(\beta';\mathbf{0})_{n,q}\}]^{5} \qquad (10)$$

is formed, with $\mathrm{Re}\{.\}$ and $\mathrm{Im}\{.\}$ as the real and imaginary parts, respectively.
Step 2: The statistic

$$\mathcal{T}^{(K)}_{n,q} = K\hat{\mathbf{c}}^{(K)}_{r^{(i)},n,q}\,\hat{\boldsymbol{\Sigma}}^{-1}_{r^{(i)},n,q}\,\hat{\mathbf{c}}^{(K)\dagger}_{r^{(i)},n,q}{}^{5} \qquad (11)$$

is computed for the tested candidate CF, β'. Here $\dagger$ and -1 denote matrix transpose and inverse, respectively, and $\hat{\boldsymbol{\Sigma}}^{-1}_{r^{(i)},n,q}$ is an estimate of the matrix

$$\boldsymbol{\Sigma}_{r^{(i)},n,q} = \begin{bmatrix} \mathrm{Re}\{(Q_{2,0}+Q_{2,1})/2\} & \mathrm{Im}\{(Q_{2,0}-Q_{2,1})/2\} \\ \mathrm{Im}\{(Q_{2,0}+Q_{2,1})/2\} & \mathrm{Re}\{(Q_{2,0}-Q_{2,1})/2\} \end{bmatrix}^{5}, \qquad (12)$$

where
$Q_{2,0} := \lim_{K\to\infty} \mathrm{Cum}[\hat{c}^{(K)}_{r^{(i)}}(\beta';\mathbf{0})_{n,q}, \hat{c}^{(K)}_{r^{(i)}}(\beta';\mathbf{0})_{n,q}]^{5}$,
and $Q_{2,1} := \lim_{K\to\infty} \mathrm{Cum}[\hat{c}^{(K)}_{r^{(i)}}(\beta';\mathbf{0})_{n,q}, \hat{c}^{(K)*}_{r^{(i)}}(\beta';\mathbf{0})_{n,q}]^{5}$,
with $\mathrm{Cum}[.]$ as the cumulant operator[6]. The covariances $Q_{2,0}$ and $Q_{2,1}$ are given respectively by[7,8] [12]

$$Q_{2,0} = \lim_{K\to\infty} K^{-1}\sum_{k=0}^{K-1}\sum_{\xi=-\infty}^{\infty} \mathrm{Cum}[L_{r^{(i)}}(k;\mathbf{0})_{n,q}, L_{r^{(i)}}(k+\xi;\mathbf{0})_{n,q}] \times e^{-j2\pi 2\beta' k} e^{-j2\pi\beta'\xi},$$

and

$$Q_{2,1} = \lim_{K\to\infty} K^{-1}\sum_{k=0}^{K-1}\sum_{\xi=-\infty}^{\infty} \mathrm{Cum}[L_{r^{(i)}}(k;\mathbf{0})_{n,q}, L^{*}_{r^{(i)}}(k+\xi;\mathbf{0})_{n,q}] \times e^{-j2\pi(-\beta')\xi},$$

where $L_{r^{(i)}}(k;\mathbf{0})_{n,q} := \prod_{u=1}^{n} r^{(i)(*)_u}(k)$ is the nth-order/ q-conjugate lag product of $r^{(i)}(k)$, for zero delay-vector, with $(*)_u$, $u = 1,...,n$, as a possible conjugation, so that the total number of conjugations is q.
Step 3: The statistic $\mathcal{T}^{(K)}_{n,q}$ [5], estimated at tested candidate CF β' and for zero delay, is compared against a threshold, $\Gamma^{(l)}$, $l = 1,...,4$, for decision-making. If $\mathcal{T}^{(K)}_{n,q} \geq \Gamma^{(l)}$ [5], one decides that the tested candidate CF is indeed a CF for zero delay; otherwise it is not declared a CF. The threshold is set for a given probability of false alarm, $P_F^{(l)} = \Pr\{\mathcal{T}^{(K)}_{n,q} \geq \Gamma^{(l)} \mid H_0\}$ [5], $l = 1,...,4$, by taking into account that $\mathcal{T}^{(K)}_{n,q}$ [5] has an asymptotic χ^2 distribution with two degrees of freedom under H_0 [12].

IV. Simulation Results

A. Simulation Setup

For the generation of analog signals, the modulating signal $x(t)$ is obtained by low-pass filtering a sequence of zero-mean Gaussian random numbers, with unit variance. The analog signals

[4] By using the cyclic cumulant-to-moment formula, along with (21)-(22) and (25)-(26), one can easily prove that the magnitude of the sixth-order/ three-conjugate CTMF at $\beta = \pm f_s^{-1}/T$ is greater than that of the second-order/ one-conjugate CTCF at the same CFs.

[5] For Node 1 $n = 1$ and $q = 0$, for Node 2 $n = 2$ and $q = 0$, and for Nodes 3 and 4 $n = 2$, and $q = 1$.

[6] For the cumulant definition, see, e.g., [13], Ch.2.

[7] Note that these equalities are always valid if $n = 1$, whereas only for a zero-mean process if $n = 2$.

[8] For the covariance estimators, see, e.g., [12], eq. (48).

are scaled so that the signal power is 1. For the AM signal, the modulation index μ_A is randomly chosen between 0 and 1. For the linear digital modulation class, we simulate BPSK, QPSK, 8-PSK, 16-QAM and 64-QAM, with unit variance constellations. The signal power is also set to 1, and the pulse shape $p_{TX}(t)$ is root-raised cosine, with 0.25 roll-off factor [10]. The signal bandwidth is $B = 3$ KHz. At the receive-side, a low-pass filter is used to eliminate the out-of-band noise, and the received signal is sampled at a rate $f_s = 48$ KHz. The observation interval available at the receiver is 1 second, which yields $K = 4.8\times 10^4$ samples. The SNR is defined as the signal power to the noise power at the output of receive filter. All received signals are affected by a phase θ, uniformly distributed over $[-\pi,\pi)$, and a carrier frequency offset, $\Delta f_c f_s^{-1} = 0.01$. In addition, linear digital signals are affected by a timing error εT, with ε=0.8.

B. Estimated CTCF Magnitude, Statistic Used for Decision-Making and Threshold Setting

The magnitudes of the first-order/ zero-conjugate CTCFs of AM and BPSK signals are given for illustration in Fig. 2 a) and b), at -10dB and -20dB SNR, respectively. For AM, one can notice the peak in $|\hat{c}^{(K)}_{r^{(\mathrm{AM})}}(\beta')_{1,0}|$ at $\beta' = \beta = \Delta f_c f_s^{-1} = 0.01$, as well as the reduction of its value with a decrease in SNR. On the other hand, non-zero spikes due to estimation based on a finite length data sequence are to be noted in $|\hat{c}^{(K)}_{r^{(i)}}(\beta')_{1,0}|$, i=AM and DSB.

Based on $\hat{c}^{(K)}_{r^{(i)}}(\beta';0)_{n,q}$ [5], the statistic $\mathcal{T}^{(K)}_{n,q}$ [5] is calculated at each node l, $l=1,\ldots,4$, according to (11). A Kaiser window of length 61 and parameter 10 was used to compute the covariance estimates in (12)[8]. At each node l, the statistic is compared against a threshold, $\Gamma^{(l)}$, $l=1,\ldots,4$. Here $\Gamma^{(1)} = \Gamma^{(2)} = 18.412$, and $\Gamma^{(3)} = \Gamma^{(4)} = 13.816$. These values correspond to a probability of false alarm of 10^{-4} and 10^{-3}, respectively [14], and are set based on the estimated values of the statistics used for decision-making.

C. Classification Performance

To evaluate the performance of the proposed classification algorithm, we define the average probability of correct classification at each node l, $l=1,\ldots,4$, as $P^{(l)}_{cc} = 2^{-1}\sum_{l_i=1}^{2} P^{(l_i|l_i)}_{cc}$, with $P^{(l_i|l_i)}_{cc}$ as the average probability to choose the branch l_i, $l_i = 1,\ 2$, when indeed the branch l_i is the correct choice. The probability $P^{(l_i|l_i)}_{cc}$ is further computed as $\sum_{i=1}^{N^{(l_i)}_{\mathrm{mod}}} P^{(l_i|i)}_{c} / N^{(l_i)}_{\mathrm{mod}}$, with $N^{(l_i)}_{\mathrm{mod}}$ as the number of possible modulations for the l_i th branch, and $P^{(l_i|i)}_{c}$ as the probability to choose the l_i th branch when the i th signal is transmitted, $i=1,\ldots,N^{(l_i)}_{\mathrm{mod}}$. For example, with $l=1$ (Node 1) and $l_1 = 1$ (AM branch), $N^{(1)}_{\mathrm{mod}} = 1$, and $P^{(1|1)}_{cc} = P^{(1|1)}_{c}$. The $P^{(l_i|i)}_{c}$ is estimated based on 300 Monte Carlo trials.

The average probability of correct classification at each node of the proposed binary decision tree algorithm, $P^{(l)}_{cc}$, $l=1,\ldots,4$, is plotted versus SNR in Fig. 3. At Node 1 ($l=1$), a probability of correct classification of one is achieved at SNRs as low as -23dB, to discriminate AM from DSB, SSB, BPSK, QPSK, 8-PSK, 16-QAM and 64-QAM. At Node 2 ($l=2$), such a performance is attained as SNRs as low as -8dB, to discriminate DSB and BPSK from SSB, QPSK, 8-PSK, 16-QAM, and 64-QAM. At Nodes 3 and 4 ($l=3,\ 4$), 5dB SNR is required to discriminate with probability one between DSB and BPSK, and SSB and QPSK, 8-PSK, 16-QAM and 64-QAM, respectively.

Note that the statistic $\mathcal{T}^{(K)}_{2,1}$, which is currently used at Nodes 3 and 4, can be applied to distinguish between analog and digital modulations at Node 1, i.e., to discriminate AM, DSB and SSB from *M*-PSK and *M*-QAM. However, higher SNR would be required to achieve the same classification performance at Node 1, and, thus, the performance of the whole classifier would be limited. It is also to be noted that results previously presented are achieved for 1 second observation interval. Apparently, if a larger observation interval is available at the receive-side, the estimates will be more accurate, which in turn will result in a better classification performance.

V. CONCLUSION

A cyclostationarity-based binary decision tree algorithm has been proposed for analog and digital modulation classification. The algorithm provides a good classification performance in additive Gaussian noise, and does not require estimation of carrier phase and frequency offset, signal and noise powers, and timing recovery in the preprocessing step.

REFERENCES

[1] O. A. Dobre, A. Abdi, Y. Bar-Ness, and W. Su, “A survey of automatic modulation classification techniques: Classical approaches and new trends,” to be published in *IEE Proc. Commun*., 2006.

[2] O. A. Dobre, Y. Bar-Ness, and W. Su, “Higher-order cyclic cumulants for high order modulation classification,” in *Proc. IEEE MILCOM*, 2003, pp. 112-117.

[3] C. M. Spooner, “Classification of cochannel communication signal using cyclic cumulants”, *in Proc. ASILOMAR*, 1995, pp. 531-536.

[4] O. A. Dobre, A. Abdi, Y. Bar-Ness, and W. Su, “Selection combining for modulation recognition in fading channels,” in *Proc. IEEE MILCOM*, 2005, pp.1-7.

[5] E. E. Azzouz and A. K. Nandi, *Automatic Modulation Recognition of Communication Signals*. Kluwer, 1996.

[6] Y. T. Chan, L. G. Gadbois, and P. Yansouni, “Identification of the modulation type of a signal,” *Signal Process.*, vol. 16, pp. 149-154, 1989.

[7] O. A. Dobre, A. Abdi, Y. Bar-Ness, and W. Su, “The classification of joint analog and digital modulations,” in *Proc. IEEE MILCOM*, 2005, pp.1-6.

[8] Y. O. Al-Jalili, “Identification algorithm of upper sideband and lower sideband SSB signals,” *Signal Process*., vol. 42, pp. 207-213, 1995.

[9] W. A. Gardner, *Cyclostationarity in Communications and Signal Processing*. New York: IEEE Press, 1994.
[10] A. B. Carlson, P. B. Crilly, and J. C. Rutledge, *Communication Systems*, 4th ed. McGraw Hill, 2002.
[11] A. Napolitano, "Cyclic higher-order statistics: input/output relations for discrete- and continuous-time MIMO linear almost-periodically time-variant systems," *Signal Process.*, vol. 42, pp. 147-166, 1995.
[12] A. V. Dandawade and G. B. Giannakis, "Statistical tests for presence of cyclostationarity," *IEEE Trans. Signal Process.*, vol. 42, pp. 2355-2369, 1994.
[13] C. L. Nikias and A. P. Petropulu, *Higher-Order Spectra Analysis: A Nonlinear Signal Processing Framework*. Prentice Hall, 1993
[14] M. Abramowitz and I. A. Stegun, *Handbook of Mathematical Functions*. New York: Dover Publications, 1972.
[15] R. C. Cabot, "A note on the application of the Hilbert transform to time delay estimation," *IEEE Trans. Acoust., Speech, Signal Processing*, vol. 29, pp. 607-609, 1981.

APPENDIX A: TEMPORAL CYCLOSTATIONARITY PARAMETERS

In the fraction-of-time (FOT) probability framework, signals are modeled as time-series rather than realizations of stochastic processes [9], [11]. Thus, with the FOT probability approach, statistical parameters are defined through infinite-time averages rather than ensemble averages. This approach is subsequently used to present temporal cyclostationarity parameters.

Let $r^{(i)}(t)$ be a continuous-time complex-valued time-series, and $\tilde{L}_{r^{(i)}}(t;\tilde{\boldsymbol{\tau}})_{n,q}$ be the nth-order/q-conjugate lag product of $r^{(i)}(t)$, defined as

$$\tilde{L}_{r^{(i)}}(t;\tilde{\boldsymbol{\tau}})_{n,q} := \prod_{u=1}^{n} r^{(i)(*)_u}(t+\tilde{\tau}_u), \tag{13}$$

where $\tilde{\boldsymbol{\tau}} = [\tilde{\tau}_1 = 0 \ \tilde{\tau}_2 \ldots \tilde{\tau}_n]^\dagger$ is the delay-vector. The time-series $r^{(i)}(t)$ is said to be nth-order cyclostationary for a given conjugation configuration (q-conjugate) if

$$\begin{aligned}\tilde{m}_{r^{(i)}}(\tilde{\alpha};\tilde{\boldsymbol{\tau}})_{n,q} &:= \lim_{I\to\infty} I^{-1}\int_{-I/2}^{I/2} \tilde{L}_{r^{(i)}}(t;\tilde{\boldsymbol{\tau}})_{n,q} e^{-j2\pi\tilde{\alpha}t}dt \\ &:= < \tilde{L}_{r^{(i)}}(t;\tilde{\boldsymbol{\tau}})_{n,q} e^{-j2\pi\tilde{\alpha}t} >\end{aligned} \tag{14}$$

exists and is non-zero for some delay vectors and a denumerable set of real $\tilde{\alpha}$, with $\tilde{\alpha} \neq 0$ [9]. Eq. (14) defines the CTMF, with $\tilde{\alpha}$ as CF. It is to be noted that CTMF arises from a consideration of the finite-strength additive sine-wave components in the lag product. The sum of all such components is given by the temporal moment function (TMF) [9],

$$\tilde{m}_{r^{(i)}}(t;\tilde{\boldsymbol{\tau}})_{n,q} := \mathrm{E}^{\{\tilde{\alpha}\}}[\tilde{L}_{r^{(i)}}(t;\tilde{\boldsymbol{\tau}})_{n,q}] = \sum_{\tilde{\alpha}\in\tilde{\kappa}^m_{n,q}} \tilde{m}_{r^{(i)}}(\tilde{\alpha};\tilde{\boldsymbol{\tau}})_{n,q} e^{j2\pi\tilde{\alpha}t}, \tag{15}$$

where $\tilde{\kappa}^m_{n,q} = \{\tilde{\alpha} : \tilde{m}_{r^{(i)}}(\tilde{\alpha};\tilde{\boldsymbol{\tau}})_{n,q} \neq 0\}$, and $\mathrm{E}^{\{\tilde{\alpha}\}}[.]$ is the expectation operator in the FOT probability framework, which replaces the usual operator $\mathrm{E}[.]$ in the stochastic framework. This actually performs a sine-wave extraction operation, i.e., it extracts all additive sine-wave components existent in its argument.

The nth-order/ q-conjugate temporal cumulant function (TCF) of $r^{(i)}(t)$ can be expressed in terms of the nth- and lower-order TMFs by using the moment-to-cumulant formula [9],

$$\begin{aligned}\tilde{c}_{r^{(i)}}(t;\tilde{\boldsymbol{\tau}})_{n,q} &:= \mathrm{Cum}[r^{(i)(*)_1}(t) \ldots r^{(i)(*)_{n-1}}(t+\tilde{\tau}_{n-1}) r^{(i)(*)_n}(t+\tilde{\tau}_n)] \\ &= \sum_{\{\wp_1,\ldots,\wp_Z\}} (-1)^{Z-1}(Z-1)! \prod_{z=1}^{Z} \tilde{m}_{r^{(i)}}(t;\tilde{\boldsymbol{\tau}}_z)_{n_z,q_z},\end{aligned} \tag{16}$$

where $\{\wp_1,\ldots,\wp_Z\}$ is a partition of $\wp = \{1,2,\ldots,n\}$, with $\wp_z$, $z = 1,\ldots,Z$, as non-empty disjoint subsets of $\wp$, so that their reunion is $\wp$, Z is the number of the subsets in a partition ($1 \le Z \le n$), $\tilde{\boldsymbol{\tau}}_z$ is a delay vector whose components are elements of $\{\tilde{\tau}_u\}_{u=1}^n$, with indices specified by $\wp_z$, and n_z is the number of elements in the subset $\wp_z$, from which q_z correspond to conjugate terms. Note that $\sum_{z=1}^{Z} n_z = n$ and $\sum_{z=1}^{Z} q_z = q$. Furthermore, $\tilde{c}_{r^{(i)}}(t;\tilde{\boldsymbol{\tau}})_{n,q}$ turns out to be an almost-periodic function of time that can be written as [9]

$$\tilde{c}_{r^{(i)}}(t;\tilde{\boldsymbol{\tau}})_{n,q} = \sum_{\tilde{\beta}\in\tilde{\kappa}^c_{n,q}} \tilde{c}_{r^{(i)}}(\tilde{\beta};\tilde{\boldsymbol{\tau}})_{n,q} e^{j2\pi\tilde{\beta}t}, \tag{17}$$

where

$$\tilde{c}_{r^{(i)}}(\tilde{\beta};\tilde{\boldsymbol{\tau}})_{n,q} = \lim_{I\to\infty} I^{-1}\int_{-I/2}^{I/2} \tilde{c}_{r^{(i)}}(t;\tilde{\boldsymbol{\tau}})_{n,q} e^{-j2\pi\tilde{\beta}t}dt \tag{18}$$

is the nth-order/ q-conjugate CTCF at CF $\tilde{\beta}$, and $\tilde{\kappa}^c_{n,q} = \{\tilde{\beta} : \tilde{c}_{r^{(i)}}(\tilde{\beta};\tilde{\boldsymbol{\tau}})_{n,q} \neq 0\}$.
By using (15), (16) and (17), the nth-order/q-conjugate CTCF of $r^{(i)}(t)$ at a CF $\tilde{\beta}$ can be expressed as [9]

$$\begin{aligned}\tilde{c}_{r^{(i)}}(\tilde{\beta};\tilde{\boldsymbol{\tau}})_{n,q} &= \sum_{\{\wp_1,\ldots,\wp_Z\}} (-1)^{Z-1}(Z-1)! \\ &\times \sum_{\tilde{\boldsymbol{\alpha}}^\dagger \mathbf{1}=\tilde{\beta}} \prod_{z=1}^{Z} \tilde{m}_{r^{(i)}}(\tilde{\alpha}_z;\tilde{\boldsymbol{\tau}}_z)_{n_z,q_z},\end{aligned} \tag{19}$$

where $\tilde{\boldsymbol{\alpha}} = [\tilde{\alpha}_1 \ldots \tilde{\alpha}_Z]^\dagger$ is a set of CFs and $\mathbf{1}$ is a Z-dimensional one vector. Eq. (19) is referred to as the cyclic moment-to-cumulant formula. A similar expression can be written to express the CTMF as a function of CTCFs. This is referred to as the cyclic cumulant-to-moment formula, and is given by [9]

$$\tilde{m}_{r^{(i)}}(\tilde{\alpha};\tilde{\boldsymbol{\tau}})_{n,q} = \sum_{\{\wp_1,\ldots,\wp_Z\}} \sum_{\tilde{\boldsymbol{\beta}}^\dagger \mathbf{1}=\tilde{\alpha}} \prod_{z=1}^{Z} \tilde{c}_{r^{(i)}}(\tilde{\beta}_z;\tilde{\boldsymbol{\tau}}_z)_{n_z,q_z}, \tag{20}$$

where $\tilde{\boldsymbol{\beta}} = [\tilde{\beta}_1 \ldots \tilde{\beta}_Z]^\dagger$ is a set of CFs.

For the discrete-time signal $r^{(i)}(k) = r^{(i)}(t)|_{t=kf_s^{-1}}$, obtained by sampling the continuous-time signal $r^{(i)}(t)$ at a sampling rate f_s, the nth-order/ q-conjugate CTCF and the set of CFs are respectively given as (under the assumption of no aliasing) [11]

$$c_{r^{(i)}}(\beta;\boldsymbol{\tau})_{n,q} = \tilde{c}_{r^{(i)}}(\beta f_s;\boldsymbol{\tau} f_s^{-1})_{n,q}, \tag{21}$$

$$\kappa^c_{n,q} = \{\beta \in [-1/2;1/2) : \beta = \tilde{\beta}/f_s,\ c_{r^{(i)}}(\beta;\boldsymbol{\tau})_{n,q} \neq 0\}, \tag{22}$$

where $\boldsymbol{\tau} = \tilde{\boldsymbol{\tau}} f_s$, with components $\tau_u = \tilde{\tau}_u f_s$, $u = 1,\ldots,n$.

Estimators of the cyclostationarity parameters defined in the FOT framework are obtained by considering finite-time averages, and converge asymptotically to the true values, which are the infinite-time averages of the same quantities [9].

APPENDIX B: DERIVATIONS OF (2)-(9)

Subsequently, first- and/ or second-order temporal cyclostationarity parameters of the signals of interest are derived.

With a zero-mean purely stationary modulating signal $x(t)$ [9], by using (13) and (14) with the signal given in (1), and taking into account the statistical properties of the noise, one can easily show that the first-order/ zero-conjugate CTMFs of the received signals $r^{(i)}(t)$, $i = \text{AM, DSB, SSB}$, are as follows,

$$\tilde{m}_{r^{(\mathrm{AM})}}(\tilde{\alpha})_{1,0} := < r^{(\mathrm{AM})}(t) e^{-j2\pi\tilde{\alpha}t} >$$
$$= < e^{j\theta} e^{j2\pi\Delta f_c t} A(1+\mu_A x(t)) e^{-j2\pi\tilde{\alpha}t} > = \begin{cases} A e^{j\theta}, & \tilde{\alpha} = \Delta f_c \\ 0, & \text{otherwise} \end{cases}, \tag{23}$$

and

$$\tilde{m}_{r^{(i)}}(\tilde{\alpha})_{1,0} = 0, \ \text{any } \tilde{\alpha}, i\text{=DSB, SSB}. \tag{24}$$

As the first-order CTMF and CTCF are identical, (23) and (24) hold also for the first-order/ zero-conjugate CTCF, i.e., $\tilde{c}_{r^{(i)}}(\tilde{\beta})_{1,0} = \tilde{m}_{r^{(i)}}(\tilde{\alpha})_{1,0}$, $\tilde{\beta} = \tilde{\alpha}$, i=AM, DSB, SSB.

The n th-order/ q -conjugate CTCF of linear digital modulations is [2]-[3]

$$\tilde{c}_{r^{(i)}}(\tilde{\beta};\tilde{\boldsymbol{\tau}})_{n,q} = c_{s^{(i)},n,q} A^n T^{-1} e^{-j2\pi\tilde{\gamma}\varepsilon T} e^{j\theta(n-2q)} e^{j2\pi\Delta f_c \sum_{u=1}^{n} (-)_u \tau_u}$$
$$\times \int_{-\infty}^{\infty} \prod_{u=1}^{n} p_{TX}^{(*)_u}(t+\tilde{\tau}_u) e^{-j2\pi\tilde{\gamma}t} dt + \tilde{c}_w(\tilde{\beta};\tilde{\boldsymbol{\tau}})_{n,q}, \tag{25}$$

where $\tilde{\beta} = \tilde{\gamma} + (n-2q)\Delta f_c$, (26)

with $\tilde{\gamma} = k/T$, k integer, $c_{s^{(i)},n,q}$ is the n th-order/ q -conjugate cumulant for the signal constellation i, i=M-PSK, M-QAM, and $(-)_u$ is the optional minus sign associated with the optional conjugation $(*)_u$, $u = 1,...,n$. Note that $\tilde{c}_w(\tilde{\beta};\tilde{\boldsymbol{\tau}})_{n,q}$ in (25) is non-zero only for $n \le 2$, $q = 0,...,n$, and $\beta = 0$. For values of the n th-order $/q$ -conjugate cumulant for different linear digital modulations, $c_{s^{(i)},n,q}$ ($n = 1,...,8$, $q = 0,...,n$), see, e.g., [2]-[3]. Odd-order cumulants, $c_{s^{(i)},n,q}$ (n odd), equal zero for symmetric signal constellations [2]. Thus, with $c_{s^{(i)},1,0} = 0$, the first-order/ zero-conjugate CTCFs of M-PSK and M-QAM signals become zero, i.e., $\tilde{c}_{r^{(i)}}(\tilde{\beta})_{1,0} = 0$, any $\tilde{\beta}$, i=M-PSK, M-QAM.

Second-order cyclostationarity is subsequently investigated for DSB, SSB, M-PSK and M-QAM signals. One can easily show that the second-order/ zero-conjugate CTMFs of the received signals $r^{(i)}(t)$, i=DSB, SSB, are as follows,

$$\tilde{m}_{r^{(\mathrm{DSB})}}(\tilde{\alpha};\tilde{\tau})_{2,0} := < r^{(\mathrm{DSB})}(t) r^{(\mathrm{DSB})}(t+\tilde{\tau}) e^{-j2\pi\tilde{\alpha}t} > =$$
$$= \begin{cases} A^2 e^{j2\theta} e^{j2\pi\Delta f_c \tilde{\tau}} \tilde{m}_x(\tilde{\tau})_{2,0}, & \tilde{\alpha} = 2\Delta f_c \\ 0, & \text{otherwise} \end{cases}, \tag{27}$$

and

$$\tilde{m}_{r^{(\mathrm{SSB})}}(\tilde{\alpha};\tilde{\tau})_{2,0} := < r^{(\mathrm{SSB})}(t) r^{(\mathrm{SSB})}(t+\tilde{\tau}) e^{-j2\pi\tilde{\alpha}t} > = 0, \ \text{any } \tilde{\alpha}. \tag{28}$$

The identities $\tilde{m}_x(\tilde{\tau})_{2,0} = \tilde{m}_{\underset{\smile}{x}}(\tilde{\tau})_{2,0}$ and $\tilde{m}_{x\underset{\smile}{x}}(\tilde{\tau})_{2,0} = -\tilde{m}_{\underset{\smile}{x}x}(\tilde{\tau})_{2,0}$ [10] are used to derive (28), with $\tilde{m}_x(\tilde{\tau})_{2,0} := < x(t)x(t+\tilde{\tau}) >$, $\tilde{m}_{\underset{\smile}{x}}(\tilde{\tau})_{2,0} := < \underset{\smile}{x}(t)\underset{\smile}{x}(t+\tilde{\tau}) >$, $\tilde{m}_{x\underset{\smile}{x}}(\tilde{\tau})_{2,0} := < x(t)\underset{\smile}{x}(t+\tilde{\tau}) >$, and $\tilde{m}_{\underset{\smile}{x}x}(\tilde{\tau})_{2,0} := < \underset{\smile}{x}(t)x(t+\tilde{\tau}) >$.

As the first-order CTMF equals zero for $i = \text{DSB}$ and SSB, as well as for the noise $w(t)$, the cyclic moment-to-cumulant formula yields the equality of second-order/ zero-conjugate CTCF and CTFM, i.e., $\tilde{c}_{r^{(i)}}(\tilde{\beta};\tilde{\tau})_{2,0} = \tilde{m}_{r^{(i)}}(\tilde{\alpha};\tilde{\tau})_{2,0}$, $\tilde{\beta} = \tilde{\alpha}$, $i = \text{DSB, SSB}$.

By applying (25), with $n = 2$, $q = 0$, $\tilde{\boldsymbol{\tau}} = [0, \tilde{\tau}]^{\dagger}$, and $c_{s^{(i)},2,0}$ =1 for i=BPSK and $c_{s^{(i)},2,0}$ =0 for i=M-PSK and M-QAM, $M \ge 4$ [2], the second-order/ zero-conjugate CTCFs of M-PSK and M-QAM signals are found as

$$\tilde{c}_{r^{(i)}}(\tilde{\beta};\tilde{\tau})_{2,0} = \begin{cases} A^2 T^{-1} e^{-j2\pi\tilde{\gamma}\varepsilon T} e^{j2\theta} e^{j2\pi\Delta f_c \tilde{\tau}} \\ \times \int_{-\infty}^{\infty} p_{TX}(t) p_{TX}(t+\tilde{\tau}) e^{-j2\pi\tilde{\gamma}t} dt, & i = \text{BPSK} \\ 0, \quad i = M\text{-PSK}, M\text{-QAM}, M \ge 4, \end{cases} \tag{29}$$

where $\tilde{\beta} = \tilde{\gamma} + 2\Delta f_c$, with $\tilde{\gamma} = k/T$, k integer.

Similarly, one can show that the second-order/ one-conjugate CTMFs of the DSB and SSB signals are given respectively as,

$$\tilde{m}_{r^{(\mathrm{DSB})}}(\tilde{\alpha};\tilde{\tau})_{2,1} := \left\langle r^{(\mathrm{DSB})}(t) (r^{(DSB)}(t+\tilde{\tau}))^* e^{-j2\pi\tilde{\alpha}t} \right\rangle$$
$$= \begin{cases} 2A^2 e^{-j2\pi\Delta f_c \tilde{\tau}} \tilde{m}_x(\tilde{\tau})_{2,1} + \tilde{m}_w(\tilde{\alpha};\tilde{\tau})_{2,1}, & \tilde{\alpha} = 0 \\ 0, & \text{otherwise} \end{cases}, \tag{30}$$

and

$$\tilde{m}_{r^{(\mathrm{SSB})}}(\tilde{\alpha};\tilde{\tau})_{2,1} := \left\langle r^{(\mathrm{SSB})}(t) (r^{(\mathrm{SSB})}(t+\tilde{\tau}))^* e^{-j2\pi\tilde{\alpha}t} \right\rangle$$
$$= \begin{cases} 2A^2 e^{-j2\pi\Delta f_c \tilde{\tau}} (\tilde{m}_x(\tilde{\tau})_{2,1} \mp j\underset{\smile}{\tilde{m}}_x(\tilde{\tau})_{2,1}) + \tilde{m}_w(\tilde{\alpha};\tilde{\tau})_{2,1}, & \tilde{\alpha} = 0 \\ 0, & \text{otherwise} \end{cases}, \tag{31}$$

where $\tilde{m}_x(\tilde{\tau})_{2,1} := < x(t)x^*(t+\tilde{\tau}) >$ and $\underset{\smile}{\tilde{m}}_x(\tilde{\tau})_{2,1}$ is the Hilbert transform of $\tilde{m}_x(\tilde{\tau})_{2,1}$. The identity $\tilde{m}_{x\underset{\smile}{x}}(\tilde{\tau})_{2,1} = \underset{\smile}{\tilde{m}}_x(\tilde{\tau})_{2,1}$ [15], with $\tilde{m}_{x\underset{\smile}{x}}(\tilde{\tau})_{2,1} := < x(t)\underset{\smile}{x}^*(t+\tilde{\tau}) >$, is used in deriving (31). Note that $\tilde{m}_x(\tilde{\tau})_{2,1} = \tilde{m}_x(\tilde{\tau})_{2,0}$ and $\tilde{m}_{x\underset{\smile}{x}}(\tilde{\tau})_{2,1} = \tilde{m}_{x\underset{\smile}{x}}(\tilde{\tau})_{2,0}$, as $x(t)$ is a real-valued signal. By using the cyclic moment-to-cumulant formula, one can easily show that the second-order/ one-conjugate CTCFs and CTMFs of $r^{(i)}(t)$, i= DSB and SSB, are respectively equal. In other words, $\tilde{c}_{r^{(i)}}(\tilde{\beta};\tilde{\tau})_{2,1} = \tilde{m}_{r^{(i)}}(\tilde{\alpha};\tilde{\tau})_{2,1}$, $\tilde{\beta} = \tilde{\alpha}$, i= DSB, SSB.

For i=M-PSK and M-QAM, by applying (25) with $n = 2$, $q = 1$, and $c_{s^{(i)},2,1} = 1$ [2], it becomes straightforward that

$$\tilde{c}_{r^{(i)}}(\tilde{\beta};\tilde{\tau})_{2,1} = A^2 T^{-1} e^{-j2\pi\tilde{\gamma}\varepsilon T} e^{-j2\pi\Delta f_c \tilde{\tau}}$$
$$\times \int_{-\infty}^{\infty} p_{TX}(t) p_{TX}^*(t+\tilde{\tau}) e^{-j2\pi\tilde{\gamma}t} dt + \tilde{c}_w(\tilde{\beta};\tilde{\tau})_{2,1}, \tag{32}$$

with $\tilde{\beta} = \tilde{\gamma} = k/T$, k integer.

With the results previously derived for continuous-time signals, by applying (21) and (22), and taking into account signal normalization, one can easily obtain (2)-(9) for the normalized discrete-time signals.

---

[9] Based on this assumption, one can easily show that $< x(t) > = 0$ and $< x(t)x(t+\tilde{\tau})e^{-j2\pi\tilde{\alpha}t} > = < \underset{\smile}{x}(t)\underset{\smile}{x}(t+\tilde{\tau})e^{-j2\pi\tilde{\alpha}t} > = 0$, any $\tilde{\alpha} \ne 0$.

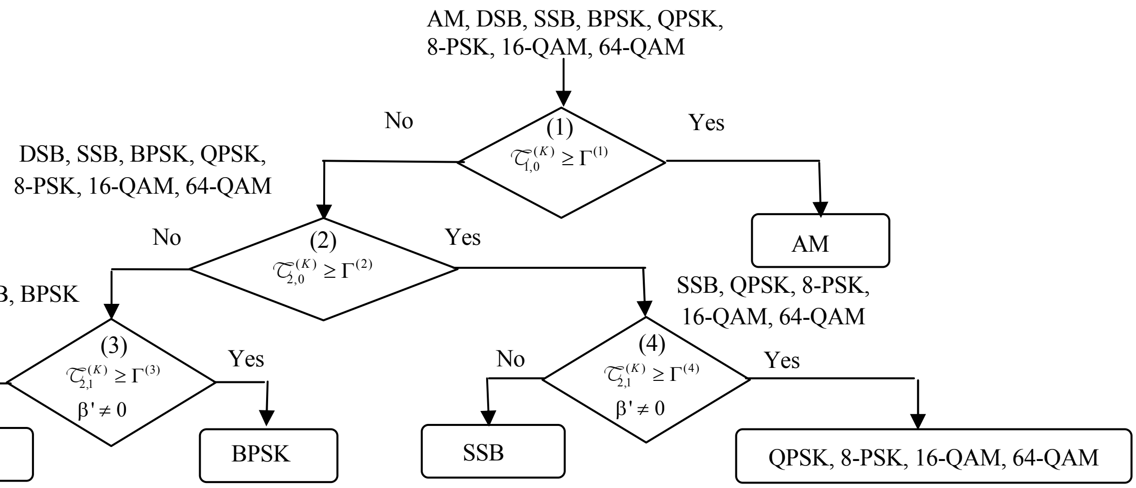

Fig. 1. Proposed cyclostationarity-based binary decision tree classification algorithm.

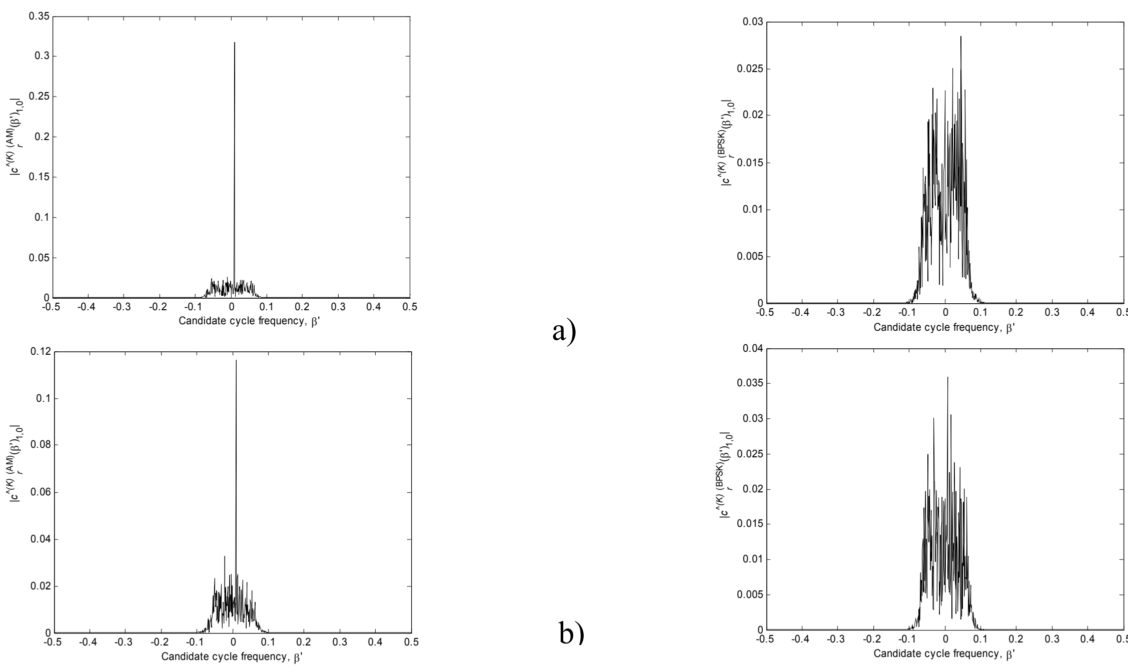

Fig. 2. The estimated first-order/ zero-conjugate CTCF magnitude of AM and BPSK signals versus candidate CFs, with $K = 4.8 \times 10^4$ samples and a) SNR=-10dB and b) SNR=-20dB.

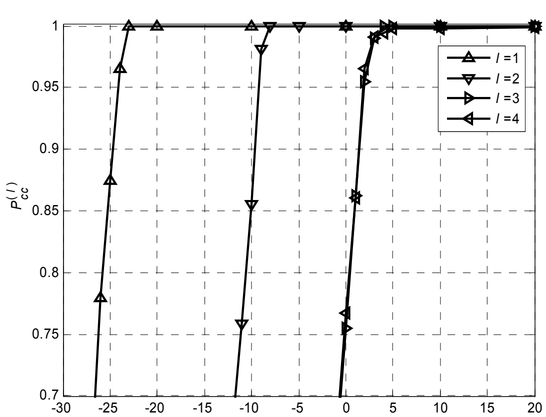

Fig. 3. The average probability of correct classification versus SNR at each node l, $l = 1,...,4$.